

Spatially redundant, precision-constrained transmit precoding for mmWave LoS MIMO

Ahmet Dundar Sezer and Upamanyu Madhow
Department of Electrical and Computer Engineering
University of California, Santa Barbara
Santa Barbara, California 93106
Email: {adsezer, madhow}@ece.ucsb.edu

Abstract—Line of sight (LoS) multi-input multi-output (MIMO) systems have attractive scaling properties with increase in carrier frequency, with the potential for 100+ Gbps links over 10s to 100s of meters with the reasonable form using the millimeter wave (mmWave) and terahertz (THz) bands. We propose and investigate an approach to all-digital LoS MIMO which addresses the difficulty of limited available precision for digital-to-analog converters (DACs) and analog-to-digital converters (ADCs). In order to reduce dynamic range requirements at the receiver, we consider spatially redundant transmit precoding (more transmit antennas than number of spatially multiplexed data streams) with 1-bit DACs. We introduce a novel approach for attaining the higher dynamic range required for precoding over the air (OTA), which we term OTA-DAC: the 1-bit DACs for clusters of transmit elements synthesize approximations to zero-forcing precoding across clusters. We illustrate our ideas for 64×4 and 16×4 LoS MIMO systems, comparing with a benchmark approach of 1-bit quantized ZF precoding for transmit elements evenly spaced across the aperture. Our OTA-DAC approach substantially outperforms the benchmark, and does not exhibit the error floors incurred by the latter.

Index Terms—Millimeter wave, LoS, MIMO, ADC, DAC.

I. INTRODUCTION

For an LoS MIMO system with a fixed form factor and link range, the available spatial degrees of freedom grow linearly and quadratically with the carrier frequency for linear and planar arrays, respectively. Given the typically linear scaling of the available signaling bandwidth with the carrier frequency, the overall data rates supported by an LoS MIMO link increase cubically with the carrier frequency. Thus, there is increasing interest in millimeter wave (mmWave) and terahertz (THz) LoS MIMO systems, leveraging recent advances in silicon-based radio frequency integrated circuits (RFICs) in these bands [1], [2].

Consider a 4×4 LoS MIMO system operating at a carrier frequency of 140 GHz with 20 GHz bandwidth and Quadrature Phase Shift Keying (QPSK) modulation. Given the link range of 100 m, 100+ Gbps data rates can be realized by such system with the transmit and receive apertures of size 0.69 meters for a linear array, and 0.11 square meters for a planar array. We wish to understand whether all-digital baseband signal processing is feasible at such high data rates. A key bottleneck is DAC and ADC precision as signal bandwidths increase. If transmit precoding is not used, we can use 1-bit DACs for a QPSK constellation, but the receiver ADCs must then provide

higher dynamic range. If transmit precoding is used, therefore eliminating the need for spatial demultiplexing at the receiver and relaxing the required ADC dynamic range, the DACs at the transmitter must support higher dynamic range. In this paper, we ask whether we can get the best of both worlds, using transmit precoding with low-precision DACs.

The opportunity: Recent promising developments in RFICs at 100+ GHz enable low-cost realization of one RF chain per antenna [3], [4], supporting all-digital MIMO with flexible configurations with a large number of antennas. We can therefore take advantage of spatial redundancy (or spatial oversampling), with many more transceiver elements than the number of spatially multiplexed data streams, to relax dynamic range requirements. We note that large inter-antenna spacings (e.g., 0.23 meters for the considered 4-fold spatial multiplexing) are required to attain the available degrees of freedom in LoS MIMO; therefore, additional antennas can be easily added to the existing aperture without changing the form factor. Recent works show that spatial redundancy at the receiver can be used to relax ADC requirements for spatial demultiplexing in LoS MIMO [5], [6]. In this paper, we investigate the potential benefits of spatial redundancy at the transmitter.

Technical approach: We consider severely quantized (1-bit in our evaluations) DACs at each transmit element. Our benchmark is a conventional strategy of computing a zero-forcing (ZF) precoder ignoring quantization, and then quantizing it at each element. We show that this naive strategy suffers from error floors. We propose an alternative approach, utilizing clusters of transmit elements: the transmit elements in each cluster are closely spaced, while the clusters are spaced across the aperture to synthesize the spatial degrees of freedom for LoS MIMO. Observing that the transmit elements in each cluster see a similar response at the receiver array, we control the 1-bit DACs to synthesize an effective symbol with larger dynamic range over-the-air: we term this approach OTA-DAC. These effective symbols approximate the output of a zero-forcing precoder across clusters. We illustrate our approach for 4-fold spatial multiplexing of QPSK data streams using 64×4 and 16×4 systems with 16 and 4 clusters spaced evenly over the aperture, respectively, with each cluster employing $\lambda/2$ -spaced transmit elements. Our benchmark scheme using the same number (64 or 16) of transmit elements, but spaces them

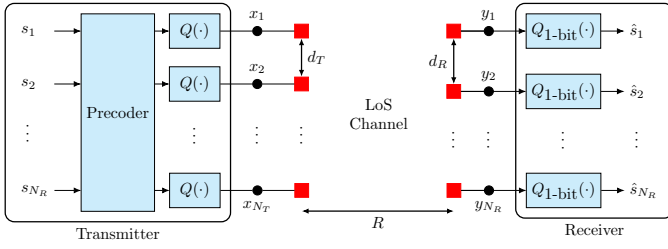


Fig. 1: Spatially redundant LoS MIMO communication system model

evenly across the aperture, and applies zero-forcing precoding quantized via 1-bit DACs at each transmit element.

Related work: The degrees of freedom for LoS MIMO systems are well known [7]–[9]. Many prior efforts for attaining these degrees of freedom focus on analog-centric [10], [11] or hybrid analog-digital [12], [13] processing, but recent work investigates all-digital receiver processing with severely quantized samples [5], [6], [14]. In [14], the proposed *virtual quantization* concept reduces ADC hardware complexity while increasing the complexity in digital processing; however still exhibits an error floor for severely quantized observations. Spatial redundancy at the receiver is shown to help relax ADC precision requirements in [5], [6]. In this paper, we show that spatial redundancy at the transmitter can be used to reduce dynamic range requirements at both the transmitter and the receiver. Since LoS MIMO is well-matched to quasi-static links (e.g., lamppost-to-lamppost or rooftop-to-rooftop backhaul communication), it is reasonable to consider precoding at the transmitter with the available channel state information [13], [15]–[17]. Our work is novel because of its combination of spatial redundancy with OTA-DAC, which we show eliminates error floors due to severe quantization.

II. SYSTEM MODEL

Consider an $N_T \times N_R$ LoS MIMO communication scheme in which an N_T -antenna transmitter with inter-antenna spacing of d_T and an N_R -antenna receiver with inter-antenna spacing of d_R are aligned with horizontal distance of R as represented in Fig. 1. Assuming each transmit/receive antenna produces a highly directive beam along the LoS, multipath is ignored. We consider the same aperture (i.e., form factor) for both the transmitter and the receiver; that is, $(N_T - 1)d_T = (N_R - 1)d_R$ with $N_T > 1$ and $N_R > 1$. For given N_R , we set the inter-antenna spacing of the receive antennas to

$$d_R = \sqrt{\frac{\lambda R}{N_R}}. \quad (1)$$

We allow N_T to vary such that $N_T \geq N_R$, and set

$$d_T = \frac{d_R(N_R - 1)}{N_T - 1}. \quad (2)$$

Based on the system model in Fig. 1, the received signal vector $\mathbf{y} \triangleq [y_1 \cdots y_{N_R}]^T \in \mathbb{C}^{N_R \times 1}$ is given by

$$\mathbf{y} = \mathbf{H}\mathbf{x} + \mathbf{n}, \quad (3)$$

where $\mathbf{x} \triangleq [x_1 \cdots x_{N_T}]^T \in \mathbb{C}^{N_T \times 1}$ is the transmitted precoded vector, $\mathbf{H} \in \mathbb{C}^{N_R \times N_T}$ is the normalized channel matrix, and $\mathbf{n} \sim \mathcal{CN}(0, \sigma^2 \mathbf{I}_{N_R})$ is AWGN.

Given $R \gg (N_T - 1)d_T = (N_R - 1)d_R$, the path loss differences among the transmit-receive pairs can be ignored and the channel between transmit antenna n and receive antenna m is given by

$$\mathbf{H}(m, n) = e^{-j\Phi} e^{-j\theta_{m,n}}, \quad (4)$$

where the random variable Φ denotes the common phase change along the path between the transmitter and the receiver and is assumed to be uniformly distributed over $[0, 2\pi)$, and

$$\theta_{m,n} \approx \frac{\pi((n-1)d_T - (m-1)d_R)^2}{\lambda R}, \quad (5)$$

for $R \gg (N_T - 1)d_T = (N_R - 1)d_R$ with λ denoting the carrier wavelength.

Precoding: The transmitter uses the available channel state information (i.e., the knowledge of the channel matrix \mathbf{H} with $\theta_{m,n}$ in (4)) to precode the transmitted signal vector $\mathbf{s} \triangleq [s_1 \cdots s_{N_R}]^T \in \mathbb{C}^{N_R \times 1}$ into the precoded vector. We do not account for the common phase $\Phi = \phi$ in transmit precoding: in practice, time variations in this phase (e.g., due to oscillator drift between the transmitter and receiver) may be too rapid to track at the transmitter via low-rate channel feedback. The transmitter is assumed to have perfect information regarding $\theta_{m,n}$ for all transmit-receive antenna pairs via feedback from the receiver and assumes that $\Phi = 0$. We consider QPSK modulation. For QPSK modulation, $\{s_i\}_{i=1}^4$ are independent and identically distributed symbols taking values $\{e^{j\pi/4}, e^{j3\pi/4}, e^{j5\pi/4}, e^{j7\pi/4}\}$ with equal probability.

Quantizer at the transmitter: While we focus on 1-bit DACs (on I and Q) for our proposed approach, we also provide results for higher precision quantization for comparison. We model the low precision DACs at the transmitter as symmetric mid-rise uniform quantizers. We consider b-bit identical regular I/Q quantizers at each transmit antenna. We set the quantization thresholds in order to minimize the distortion between the quantized and unquantized vector under the assumption that the per-antenna input to quantizers is zero-mean circularly-symmetric complex Gaussian distributed with variance P/N_T (i.e., $\mathcal{CN}(0, P/N_T)$), where P is the average power constraint at the transmitter. It is important to note that the average power is not conserved in general after the quantization; therefore, the output of the quantizer is assumed to be scaled appropriately to satisfy the average power constraint at the transmitter. We define SNR (per receive element) as $\text{SNR} = P/\sigma^2$, normalizing the propagation gain to unity.

Quantizer at the receiver: We consider 1-bit quantizers per I/Q at each receive antenna, which simply act as slicers for detecting the QPSK symbols in our system. In doing so, we implicitly assume that any common phase rotation in the constellations seen at the receive antennas has been eliminated. This can be accomplished at the receiver via a number of techniques compatible with low-precision ADC, such as

analog derotation prior to quantization [18], or phase-only quantization [19] with more than four quadrants. We do not incorporate such techniques in our modeling or performance analysis, in order to maintain focus on precision-constrained transmit precoding. Thus, we set $\Phi = 0$ for the remainder of this paper.

Considering the quantizers at the receiver as QPSK slicers and focusing on linear precoding, the precoder \mathbf{P} is obtained by minimizing the mean square error between the transmitted symbol \mathbf{s} and the received signal as follows:

$$\begin{aligned} \min_{\mathbf{P} \in \mathbb{C}^{N_T \times N_R}} \mathbb{E}_{\mathbf{s}} \left[\|\mathbf{s} - \mathbf{H}\mathbf{Q}(\mathbf{P}\mathbf{s})\|^2 \right] \\ \text{subject to } \mathbb{E}_{\mathbf{s}} \left[\|\mathbf{x}\|^2 \right] \leq P \end{aligned} \quad (6)$$

where $\mathbf{x} = \mathbf{Q}(\mathbf{P}\mathbf{s})$ is the quantized precoded vector with quantizer function $\mathbf{Q}(\cdot)$ at the transmitter.

III. OTA-DAC

In this section, we present our OTA-DAC approach in which we consider multiple clusters spaced evenly across the aperture, with each cluster having (possibly $\lambda/2$ -spaced) transmit elements with 1-bit DACs. The closely spaced elements with 1-bit DACs in the clusters approximately synthesize the outputs of the ZF precoding across clusters. In the next, we explain the ZF precoder for the clusters first, then discuss how the 1-bit DACs in the clusters are set in our OTA-DAC approach to synthesize the ZF precoded outputs with larger dynamic range.

ZF precoding: It is difficult to solve the optimization problem in (6) due to the non-linear characteristics of the quantizer function $\mathbf{Q}(\cdot)$. Therefore, instead of solving (6) directly, we consider a low complexity alternative. We first obtain the linear precoder by assuming that DACs at the transmitter have infinite precision; that is $\mathbf{x} = \mathbf{Q}(\mathbf{x})$, then quantize the resulting precoded vector based on the precoder. Therefore, as a solution to the optimization problem in (6), the zero forcing (ZF) precoder can be obtained as

$$\mathbf{P}_{\text{ZF}} = \frac{1}{\beta} \mathbf{H}^\dagger (\mathbf{H}\mathbf{H}^\dagger)^{-1} \quad (7)$$

where $\beta = \sqrt{\text{tr}((\mathbf{H}\mathbf{H}^\dagger)^{-1})/P}$ is the scaling factor to satisfy the average transmit power constraint. For the benchmark approach of the quantized ZF precoding, the quantized precoded vector can be calculated as $\mathbf{x}_{\text{ZF}} = \mathbf{Q}(\mathbf{P}_{\text{ZF}}\mathbf{s})$. It is important to note that the ZF precoder provided in (7) does not depend on the precision of the quantizers (i.e., DACs) at the transmitter.

OTA-DAC: Considering the higher dynamic range of the precoded vector at the transmitter for the clusters before quantization compared to that of the transmit symbol vector, employing 1-bit DACs directly at each transmit antenna to quantize the linear precoded vector is not sufficient to obtain acceptable performance (see Fig. 3). Motivated by the fact that the signals transmitted from the very close positioned (possibly $\lambda/2$ -spaced) transmit antennas in LoS MIMO experience almost the same channel response (i.e., θ) given $R \gg (N_T - 1)d_T$ in our model, we consider a cluster with 4 transmit antennas,

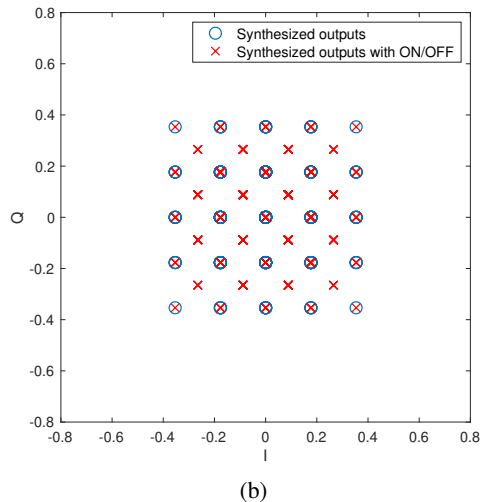
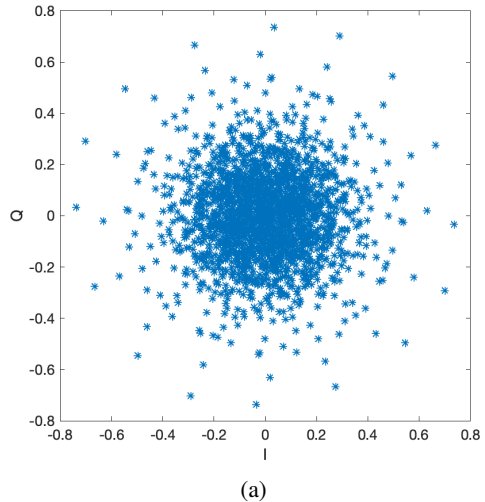


Fig. 2: (a) All possible precoded symbols for 16 clusters based on the ZF precoding before quantization, (b) All possible outputs that can be synthesized using 4 antennas in a cluster for a 64×4 LoS MIMO.

the 1-bit quantized outputs of which can be combined over the air to synthesize the required precoded vector output as much as possible. Therefore, instead of employing equally-spaced N_T transmit antennas at the transmitter, we propose a concept in which $N_T/4$ clusters, each with 4 antennas, are evenly spaced across the aperture and the 1-bit quantized outputs of 4 elements at each cluster are appropriately set to form the precoded transmit vector of $N_T/4$ clusters as far as possible with the help of the channel response.

In order to obtain the precoded vector outputs for $N_T/4$ clusters, we apply the ZF precoder in (7) across the clusters (treating existing clusters as transmit elements) based on the mathematical model discussed in Section II with $\mathbf{H} = \mathbf{H}_{\mathbf{c}}$, where $\mathbf{H}_{\mathbf{c}}$ denotes the LoS MIMO channel between the clusters at the transmitter and the receive antennas. As an example, all possible precoded symbols for 16 clusters based on the ZF precoding before quantization is shown in Fig. 2a

for a 64×4 LoS MIMO system.

Considering 1-bit DACs at the transmitter, the quantizer output at the single transmit antenna is given by

$$Q(\mathbf{u}) = \sqrt{\frac{P}{2N_T}} (\text{sgn}(\Re(\mathbf{u})) + j\text{sgn}(\Im(\mathbf{u}))) \quad (8)$$

where $\text{sgn}(\cdot)$ is the signum function, and $\Re(\mathbf{u})$ and $\Im(\mathbf{u})$ respectively denote the real and imaginary parts of a complex vector \mathbf{u} . Therefore, the set of possible quantization outputs per transmit antenna is $\mathcal{O} = \{\sqrt{P/(2N_T)}(\pm 1 \pm j)\}$.

Given the possible outputs of a single antenna, 4 transmit antennas in the cluster can synthesize 256 possible outputs. Ignoring the inter-antenna spacing between the antennas in a cluster for the ease of exposition, we show all possible outputs that can be synthesized using 4 antennas in Fig. 2b for a 64×4 LoS MIMO (see blue \circ symbols). We note that some of the combinations of antenna outputs results in the same synthesized output; therefore, the number of the possible outputs seen in Fig. 2b is less than 256. If we are allowed to turn some antennas off, then the number of the possible outputs that 4 transmit antennas can synthesize increases (see red \times symbols in Fig. 2b).

Given the precoded vector output of a cluster based on ZF precoding before quantization, our proposed OTA-DAC approach selects the closest possible output that 4 antennas can synthesize to the given precoded output and set the 1-bit outputs of the antennas accordingly. For example, in order to generate the output at top right corner in Fig. 2b, it sets the outputs of all transmit antennas in the cluster to $\sqrt{P/(2N_T)}(1+j)$. As an another example, in order to produce the output, second from top right, the outputs of three transmit antennas are set to $\sqrt{P/(2N_T)}(1+j)$ and the output of the remaining transmit antenna is set to $\sqrt{P/(2N_T)}(-1+j)$. For all possible synthesizable outputs, the corresponding 1-bit output settings for 4 transmit antennas in a cluster can be stored in a look-up table and easily retrieved when desired. It is important to emphasize that the cluster antenna settings alter when the transmitted symbol vector is changed and the OTA-DAC approach that we propose in this study is non-linear.

IV. NUMERICAL RESULTS

In this section, we evaluate the performance of our proposed OTA-DAC approach. We illustrate our OTA-DAC approach for 4-fold spatial multiplexing of QPSK data streams using 16×4 and 64×4 LoS MIMO systems, in which we, respectively, consider 4 and 16 clusters evenly spaced across the aperture, each cluster with 4 transmit antennas with the corresponding 1-bit DACs. As a benchmark for comparison, we consider the quantized ZF precoding scheme where all the transmit antennas are spaced evenly across the aperture. We note that all the scenarios illustrated have the same aperture for both the transmitter and the receiver, and the same average power constraint. In Fig. 3a and Fig. 3b, we plot bit error rate (BER) vs SNR for the ZF precoding benchmark and our OTA-DAC approach for 16×4 and 64×4 LoS MIMO systems, respectively. We see that the benchmark of ZF precoding with 1-bit

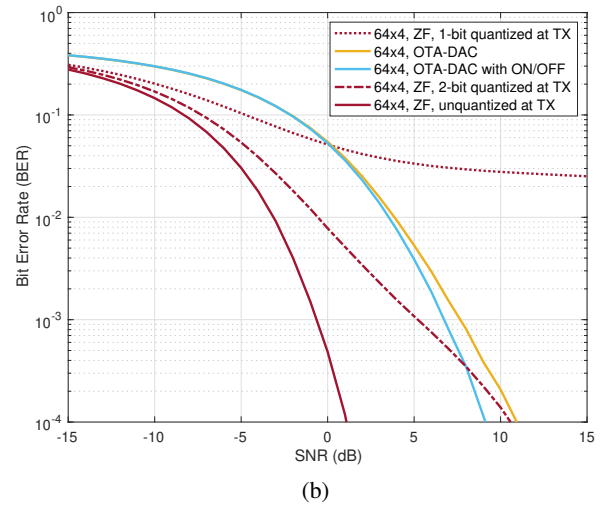
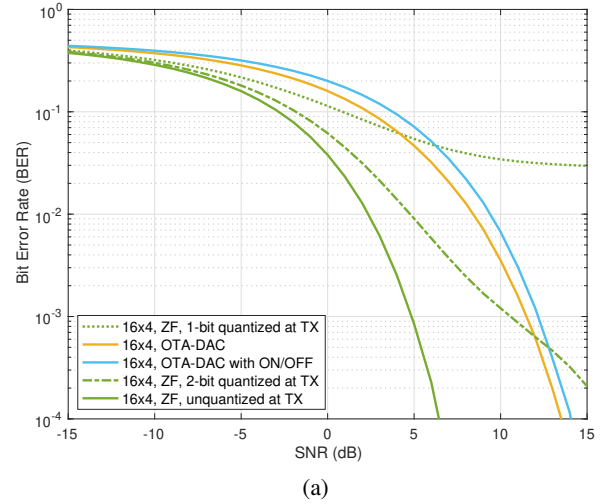


Fig. 3: Bit error rate versus SNR for ZF precoding and our proposed OTA-DAC for (a) 16×4 LoS MIMO and (b) 64×4 LoS MIMO.

quantization (i.e., 1-bit DACs) performs significantly worse for both systems, with an error floor that stays higher than the BER of 10^{-3} for which the reliable communication can be obtained via lightweight, high-rate error correcting codes. When 2-bit quantization is considered with the ZF precoding at the transmitter, the BER performance of the benchmark improves, achieving the target 10^{-3} BER at approximately 10 dB and 5 dB for 16×4 and 64×4 , respectively, but still showing the slowing-down trend at high SNR.

Refocusing our attention on 1-bit DACs at the transmitter, our proposed OTA-DAC approach performs significantly better and eliminates the error floor incurred by the 1-bit quantized ZF precoding benchmark. For 16×4 and 64×4 LoS MIMO systems, our OTA-DAC can achieve the target 10^{-3} BER at approximately 12 dB and 7 dB, respectively. It is important to note that the approximate 5 dB SNR difference among the LoS MIMO systems to achieve the target 10^{-3} BER is consisted with the expected approximate 4-fold (i.e., 6 dB) beamforming

gain (i.e., array gain) due to the 4-fold increase in the number of clusters at the transmitter given the same average power constraint for both systems and the non-optimal inter-cluster spacing for the considered spatial redundancy.

Now, we present the performance of our OTA-DAC approach with a slight modification in which we allow the transmit antennas to be turned off when desired. As seen in Fig. 3b, allowing transmit elements in the clusters to be turned off boosts the BER performance at high SNR for the 64×4 LoS MIMO system. Our OTA-DAC approach with on/off achieves the same 10^{-3} BER at approximately 6 dB, requiring 1 dB less compared to that of OTA-DAC without on/off. On the other hand, the OTA-DAC with on/off cannot outperform the standard OTA-DAC without on/off for the 16×4 LoS MIMO system as shown in Fig. 3a. Therefore, it remains an open issue as to how to optimize the set of possible outputs that can be synthesized using the transmit antennas in the clusters to enhance the BER performance further.

V. CONCLUSION

The emerging availability of mmWave RFICs with one RF chain per antenna, together with advances in packaging, enable innovations in all-digital LoS MIMO that take advantage of flexible antenna configurations. In particular, we show in this paper that spatial redundancy, together with OTA-DAC, can be used to significantly reduce dynamic range at both the transmitter and receiver. For the 16×4 and 64×4 LoS MIMO systems considered, our OTA-DAC approach significantly outperforms quantized ZF precoding (which may be viewed as a special case of OTA-DAC with a single antenna per cluster), and eliminates the error floor incurred by the latter.

The performance evaluation performed here considers relatively small clusters (4 elements) for OTA-DAC, implementing ZF-precoding across clusters. Further work is required to investigate how clusters with a larger number of elements, combining beamforming with OTA-DAC, can be employed for more challenging link budgets and larger constellations. It is also important to explore the impact of intersymbol and cross-stream interference due to misalignment [20] for severely quantized LoS MIMO. An interesting open problem is to derive computationally tractable information-theoretic benchmarks for LoS MIMO systems which are severely quantized at both transmitter and receiver.

ACKNOWLEDGMENT

This work was supported in part by ComSenTer, one of six centers in JUMP, a Semiconductor Research Corporation (SRC) program sponsored by DARPA. Use was made of computational facilities purchased with funds from the National Science Foundation (CNS-1725797) and administered by the Center for Scientific Computing (CSC). The CSC is supported by the California NanoSystems Institute and the Materials Research Science and Engineering Center (MRSEC; NSF DMR 1720256) at UC Santa Barbara.

REFERENCES

- [1] Ericsson Press Release, “Deutsche Telekom and Ericsson top 100Gbps over microwave link,” May 2019. [Online]. Available: <https://www.ericsson.com/en/press-releases/2019/5/deutsche-telekom-and-ericsson-top-100gbps-over-microwave-link>
- [2] C. B. Czegledi, M. Hörberg, M. Sjödin, P. Ligander, J. Hansryd, J. Sandberg, J. Gustavsson, D. Sjöberg, D. Polydorou, and D. Siomos, “Demonstrating 139 Gbps and 55.6 bps/Hz spectrum efficiency using 8x8 MIMO over a 1.5-km link at 73.5 GHz,” in *2020 IEEE/MTT-S International Microwave Symposium (IMS)*, 2020, pp. 539–542.
- [3] A. Simsek, S.-K. Kim, and M. J. Rodwell, “A 140 Ghz MIMO transceiver in 45 nm SOI CMOS,” in *2018 IEEE BiCMOS and Compound Semiconductor Integrated Circuits and Technology Symposium (BCICTS)*, 2018, pp. 231–234.
- [4] A. A. Farid, A. Simsek, A. S. H. Ahmed, and M. J. W. Rodwell, “A broadband direct conversion transmitter/receiver at D-band using CMOS 22nm FDSOI,” in *2019 IEEE Radio Frequency Integrated Circuits Symposium (RFIC)*, 2019, pp. 135–138.
- [5] A. D. Sezer, U. Madhow, and M. J. W. Rodwell, “Spatial oversampling for quantized LoS MIMO,” in *2021 55th Asilomar Conference on Signals, Systems, and Computers*, 2021, pp. 405–409.
- [6] T. Haelsig and B. Lankl, “Spatial oversampling in LOS MIMO systems with 1-bit quantization at the receiver,” in *SCC 2017; 11th International ITG Conference on Systems, Communications and Coding*, 2017, pp. 1–6.
- [7] F. Bohagen, P. Orten, and G. E. Oien, “Design of optimal high-rank line-of-sight MIMO channels,” *IEEE Transactions on Wireless Communications*, vol. 6, no. 4, pp. 1420–1425, 2007.
- [8] E. Torkildson, U. Madhow, and M. Rodwell, “Indoor millimeter wave MIMO: Feasibility and performance,” *IEEE Transactions on Wireless Communications*, vol. 10, no. 12, pp. 4150–4160, Dec. 2011.
- [9] H. Do, N. Lee, and A. Lozano, “Reconfigurable ULAs for line-of-sight MIMO transmission,” *IEEE Transactions on Wireless Communications*, vol. 20, no. 5, pp. 2933–2947, 2021.
- [10] M. Sawaby, B. Mamandipour, U. Madhow, and A. Arbabian, “Analog processing to enable scalable high-throughput mm-Wave wireless fiber systems,” in *50th Asilomar Conference on Signals, Systems and Computers*, Nov. 2016, pp. 1658–1662.
- [11] Y. Yan, P. Bondalapati, A. Tiwari, C. Xia, A. Cashion, D. Zhang, Q. Tang, and M. Reed, “11-Gbps broadband modem-agnostic line-of-sight MIMO over the range of 13 km,” in *IEEE Global Communications Conference (GLOBECOM)*, 2018, pp. 1–7.
- [12] A. Khalili, S. Rini, L. Barletta, E. Erkip, and Y. C. Eldar, “On MIMO channel capacity with output quantization constraints,” in *IEEE International Symposium on Information Theory (ISIT)*, June 2018, pp. 1355–1359.
- [13] L. Zhu, S. Wang, and J. Zhu, “Adaptive beamforming design for millimeter-wave line-of-sight MIMO channel,” *IEEE Communications Letters*, vol. 23, no. 11, pp. 2095–2098, 2019.
- [14] A. D. Sezer and U. Madhow, “All-digital LoS MIMO with low-precision analog-to-digital conversion,” *IEEE Transactions on Wireless Communications*, 2022.
- [15] K. Kobayashi, T. Ohtsuki, and T. Kaneko, “Precoding for MIMO systems in line-of-sight (LOS) environment,” in *IEEE Global Telecommunications Conference*, 2007, pp. 4370–4374.
- [16] L. Zhou and Y. Ohashi, “Low complexity millimeter-wave LOS-MIMO precoding systems for uniform circular arrays,” in *IEEE Wireless Communications and Networking Conference (WCNC)*, 2014, pp. 1293–1297.
- [17] P. Ferrand and S. Yang, “Blind precoding in line-of-sight MIMO channels,” in *2016 IEEE 17th International Workshop on Signal Processing Advances in Wireless Communications (SPAWC)*, 2016, pp. 1–5.
- [18] A. Wadhwa and U. Madhow, “Near-coherent QPSK performance with coarse phase quantization: A feedback-based architecture for joint phase/frequency synchronization and demodulation,” *IEEE Transactions on Signal Processing*, vol. 64, no. 17, pp. 4432–4443, 2016.
- [19] J. Singh and U. Madhow, “Phase-quantized block noncoherent communication,” *IEEE Transactions on Communications*, vol. 61, no. 7, pp. 2828–2839, July 2013.
- [20] L. Giridhar, M. E. Rasekh, A. D. Sezer, and U. Madhow, “Adaptive space-time equalization with spatial oversampling for misaligned LoS MIMO,” in *IEEE Wireless Communications and Networking Conference (WCNC)*, 2022.